Calculations of Alpha-Particle Trajectories for Long-Range Alpha Particles Emitted in Spontaneous Fission

Y. BONEH
Nuclear Research Center, Negev, Israel
AND
Z. FRAENKEL
Weizmann Institute of Science, Rehovoth, Israel
AND
I. NEBENZAHL
The Hebrew University, Jerusalem, Israel

(Received 23 September 1966; revised manuscript received 15 December 1966)

Calculated angular and energy distributions of the α particles in long-range α-particle fission are presented. The distributions were obtained from calculated α-particle trajectories based on a three-point-charge model for the scissioning nucleus. The calculation is two dimensional, and spontaneous fission (no preferred direction) is assumed. This reduces the number of free variables of the system to seven (except for the mass ratio). The system is thus parametrized in terms of the following initial dynamical variables: the initial distance between the fission fragments, the initial position of the α particle (not restricted to the fission axis), and the initial momenta of the α particle and one of the fragments. Reasonably good agreement with the experimental distributions is obtained. The calculations support the view that the scission point moves closer to the light fragment as the mass ratio increases. They also support the assumption that at the moment of scission the fission fragments have already attained a substantial part of their final velocity.

I. INTRODUCTION

THE preceding paper[1] describes an experimental investigation of the emission of long-range α particles, LRA, in the spontaneous fission of Cf^{252}. The main purpose of the experiment was to obtain quantitative information on the configuration of the fissioning nucleus at the moment of scission from the detailed investigation of the angular and energy distribution of the α particles as a function of the α-particle energy, the total fission-fragment energy, and the fission-fragment energy ratio. It is clear that little quantitative information on the scission configuration can be obtained without comparing the experimental angular and energy distributions with the results of trajectory calculations based on a given model for the scissioning nucleus.

It may seem preferable to start from the experimentally observed angular distributions and to obtain the initial configuration at the moment of scission by calculating the particle trajectories "backwards" from the (experimentally measured) final distribution to their initial positions at the moment of scission. However, it is easily shown that such a program cannot be carried out even in principle. Hence an iteration procedure must be used. One assumes a model for the scission configuration, proceeds to calculate the α-particle trajectories, compares the results with the experimental distribution, and changes the parameters describing the initial configuration until satisfactory agreement with the experimental results is obtained. In practice, the model for the scissioning nucleus may consist of the distributions for the dynamical variables of the three fragments immediately after their separation beyond the range of the nuclear force. A dynamical theory of fission should be able to predict these distributions. Indeed they were calculated for the binary-fission process in elements lighter than radium by Nix and Swiatecki,[2] who developed a dynamical theory of fission based on the classical liquid-drop model. With suitable approximations regarding the shape of the nucleus, they were able to derive the dynamical variable distributions of the two fission fragments and obtained good agreement with experimental results to the extent that these are available. Unfortunately, the classical liquid-drop theory in its present form cannot explain basic features of the binary fission of elements as heavy as californium or uranium, let alone LRA fission. Hence the initial distributions of the kinetic variables of the three fragments must be arrived at by trial and error. In order to make the problem at all amenable to present computer techniques, the number of the dynamical variables used to describe the system of these particles must be very limited. The minimum number of variables is obtained when no internal degrees of freedom are allowed and the three fragments are assumed to behave like three point charges. In this case the total number of variables reduces to 12 for a nucleus originally at rest. (For each of the three fragments there are three spatial variables describing the position of the center of mass and three conjugate momenta, making a total of 18 variables. From this total one must subtract three variables for the conservation of linear momentum and three variables for the conservation of angular momentum.) In

[1] Z. Fraenkel, preceding paper, Phys. Rev. **156**, 1283 (1967).

[2] J. R. Nix and W. J. Swiatecki, Nucl. Phys. **71**, 1 (1965).

the case of spontaneous fission (no preferred direction) the number of free variables is further reduced to 10. Since nuclear effects are neglected and the velocities are nonrelativistic, the laws of motion are those of classical mechanics and electrostatics.

A three-point-charge calculation of the trajectories of the three fragments in LRA fission has been performed by Halpern.[3] This author also tried to estimate the error involved in assuming the fission fragments to be point charges. He did this by estimating the effect of higher multipole terms on the motion of the three particles and found that this effect could safely be neglected. The present calculation is also based on the three-point-charge approximation. In addition, it assumes, for the sake of simplicity, the momenta of the three particles to be in a plane, i.e., the calculation is two-dimensional. This simplification reduces the number of free parameters of the problem to 7 (for spontaneous fission). The latter assumption was not made by Halpern, and from his results we conclude that the restriction to two dimensions does not affect our conclusions substantially. Halpern, on the other hand, neglected the effect of the α-particle recoil on the movement of the two larger fission fragments, whereas in the present paper this effect is investigated in some detail. However, the primary purpose of the present calculation is to reproduce the experimentally observed energy and angular distributions of the α particles as presented in the preceding paper.

In Sec. II we discuss the method of calculating the trajectories of the three fragments. In Sec. III we show the dependence of the final (i.e., experimentally measured) parameters, such as the α-particle energy and its angle with respect to the fission fragments, on the initial conditions such as the initial energy and the initial angle at the moment of scission. In Sec. IV we try to determine the average initial kinetic energy of the three fragments at the moment of scission. Based on the results given in Sec. IV and some assumptions regarding the initial distributions of the various parameters, in Sec. V we calculate the final energy and angular distributions and compare them with the experimental results.[1] We summarize our conclusions in Sec. VI.

II. THE CALCULATION

The motion of the three fragments under the influence of their mutual Coulomb interaction cannot be calculated in closed form, as is well known from the similar problem of three bodies in astronomy. The trajectories must therefore be calculated numerically. We first replace the differential equations of motion by a set of difference equations, and with their aid calculate the motion of the fragments for successive time intervals Δt.

[3] I. Halpern, CERN Report, 1963 (unpublished).

The equations of motion are

$$\frac{dX_{ij}}{dt}=U_{ij}, \tag{1}$$

$$m_i\frac{dU_{ij}}{dt}=F_{ij}, \tag{2}$$

where X_{ij} is the jth coordinate X_j of the ith particle, U_{ij} the j component of the velocity U_i, and F_{ij} the j component of the force F_i acting on the ith particle, and m_i its mass. These equations are replaced by the difference equations:

$$X_{ij}{}^{n+1}=X_{ij}{}^{n}+\tilde{U}_{ij}{}^{n}\Delta t, \tag{3}$$

$$U_{ij}{}^{n+1}=\tilde{U}_{ij}{}^{n}+\frac{1}{2m_i}F_{ij}{}^{n+1}\Delta t, \tag{4}$$

where

$$\tilde{U}_{ij}{}^{n}=U_{ij}{}^{n}+\frac{1}{2m_i}F_{ij}{}^{n}\Delta t \tag{5}$$

and $F_{ij}{}^{n}$ is the j component of the force acting on particle i at the position $\mathbf{X}_i{}^{n}$

$$\mathbf{F}_i{}^{n}=e^2Z_i\sum_{k=1}^{2}Z_k\frac{\mathbf{X}_i{}^{n}-\mathbf{X}_k{}^{n}}{|\mathbf{X}_i{}^{n}-\mathbf{X}_k{}^{n}|^3}. \tag{6}$$

The subscript k refers to the two other particles, and the superscript n refers to the value of the parameter after the nth time interval.

The size of the time interval is *not* chosen to be constant. A constant time interval would result in either poor accuracy for small n (i.e., when the three fragments are still close together and their direction of motion changes rapidly), or in unnecessarily small steps for large n (when the fragments are already widely separated and their direction changes only slowly). In the present calculation, the total time t_n after n time intervals is an exponential function of n:

$$t_n=t_0e^{na}, \tag{7}$$

and hence the size of the nth time interval is given by

$$\Delta t_n=t_n-t_{n-1}=t_{n-1}(e^a-1). \tag{8}$$

It is seen that the size of the time interval t_n is a function of two free parameters, t_0 and a. The parameter t_0 determines the time scale, whereas a determines the exponential growth. Roughly speaking, the parameter t_0 determines the accuracy of the calculation at the beginning of the trajectory ($t=0$), whereas a determines the accuracy towards the end of the trajectory ($t=\infty$). t_0 and a should be so chosen that the accuracy remains more or less constant during all intervals. For

the calculations presented here we chose

$$t_0=10^{-22}\text{ sec},$$
$$a=0.1.$$

Normally the calculation is terminated after 100 time intervals, i.e., after 2.2×10^{-18} sec. By that time, the distance between the particles is more than 10^3 times their initial distance and hence their potential energy is less than 10^{-3} times the initial value. The calculation of 100 time intervals takes approximately 2 sec on a CDC 1604A computer.

Our calculation conserves rigorously the linear and angular momentum of the system. This is not true for the total energy of the system. The relative error in the value of the total energy after 100 time intervals is approximately 2×10^{-3}.

The initial conditions for the calculation were as follows: (a) The mass ratio $R=m_H/m_L$ which was assumed to be equal to the charge ratio, $R=Z_H/Z_L$, where the subscript H and L refers to the heavy and light fission fragment, respectively. We have for Cf^{252}

$$m_H+m_L=248,$$
$$Z_H+Z_L=96.$$

(b) The seven initial dynamical variables: (1) The initial distance D between the two fission fragments. The line connecting the two fragments is defined as the fission axis (x axis). (2) The initial velocity of the *heavy* fragment V_H in the direction of the fission axis (x axis). (3) The initial velocity of the two fission fragments in the y direction is for sake of simplicity assumed to be zero. The initial velocity of the light fragment is $V_L=V_HR$, i.e., the total momentum of the two fission fragments is assumed to be zero. Hence the total momentum of the system is *not* zero but equal to the initial momentum of the α particle. The error introduced by this assumption is negligible. (4) The initial distance X_0 of the α particle from the heavy fragment along the fission axis (x axis). (5) The initial distance Y_0 of the α particle from the fission axis. (6) The initial energy $E_{\alpha0}$ of the α particle. (7) The initial angle θ_0 between the direction of motion of the α particle and the direction of the light fragment.

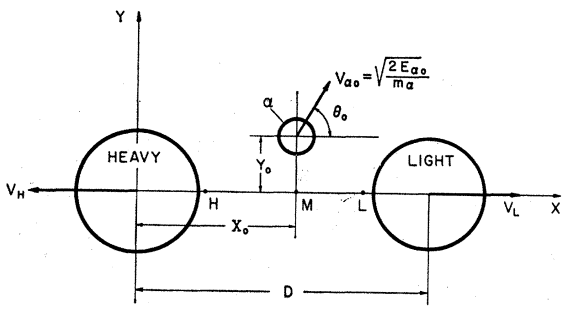

FIG. 1. Schematic diagram of the initial parameters of the calculation.

TABLE I. "Standard" set of input parameter values.

Input parameter	Symbol	Value	Unit
1 Mass ratio	R	1.4	
2 Distance between fragments	D	26.0	10^{-13} cm
3 Initial velocity of heavy fragment	V_H	0.5	10^9 cm/sec
4 Initial distance of α particle from heavy fragment	X_0	Point M	10^{-13} cm
5 Initial distance of α particle from fission axis	Y_0	0	10^{-13} cm
6 Initial energy of α particle	$E_{\alpha0}$	3.0	MeV
7 Initial angle of the α particle with respect to the fission axis	θ_0	90°	

In most of the calculations to follow, the initial position of the α particle was assumed to be *on the fission axis* ($Y_0=0$) and, in particular, at these points on that axis: Position L: At a distance of 6×10^{-13} cm from the light fragment. Position M: At the point of minimum potential energy (the saddle point of the potential-energy surface). For this point $Z_H/r_H^2=Z_L/r_L^2$, where r_i is the distance between the α particle and fission fragment i. Position H: At a distance of 6×10^{-13} cm from the heavy fragment.

Figure 1 shows a schematic diagram of the initial parameters of the calculation.

III. THE DEPENDENCE OF THE FINAL α-PARTICLE ENERGY AND ANGLE ON THE INITIAL PARAMETERS

In this section we present a set of figures showing the dependence of the final α-particle energy and angle with respect to the light-fragment direction on the various input parameters. Each graph shows the dependence on one such variable for fixed values of all other initial parameters. A single set of such "standard" values for the seven initial parameters was used for all the graphs shown in this section. This "standard" set is given in Table I. It corresponds roughly to the mean "experimental" values of the various parameters as measured (e.g., R) or as obtained from the results of the present calculation.

A. Dependence on the Initial α-Particle Energy $E_{\alpha0}$

Figure 2 shows the final α-particle energy E_α as a function of its initial energy $E_{\alpha0}$ for $Y_0=0$ and $Y_0=5\times10^{-13}$ cm. The values of all other initial parameters are those shown in Table I. Figure 2 shows a very strong dependence of the final α-particle energy on its initial value. Thus for $Y_0=0$ a variation between zero and 1.0 MeV for the initial energy corresponds to a variation between zero and 10 MeV in the value of the final energy. This "amplification" effect for the α-particle energy is a basic feature of the LRA fission process. It shows that the relatively wide experimental α-particle energy distribution may be the result of a rather narrow initial α-particle energy distribution, even if the other initial parameters have also only

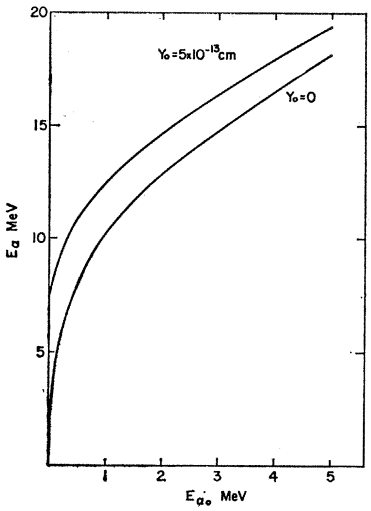

FIG. 2. The final α-particle energy E_α as a function of its initial energy $E_{\alpha 0}$. The values of the initial parameters (except for $E_{\alpha 0}$ and Y_0) are those of Table I.

relatively narrow distributions. The reason for the very strong dependence of the final α-particle energy on its initial value is the motion of the two other fission fragments. Because of this motion the force acting on the α particle is not only dependent on its position but also decreasing with time. Hence the faster the initial motion of the α particle, the larger its acceleration at any given position. Except for very small values of $E_{\alpha 0}$, there is little difference between $Y_0=0$ and $Y_0=5\times10^{-13}$ cm. The final α-particle energy E_α is zero only if both $E_{\alpha 0}$ and Y_0 are zero and X_0 corresponds to position M. In all other cases there is little dependence of E_α on Y_0 even for small values of $E_{\alpha 0}$.

B. Dependence on the Initial α-Particle Position X_0

Figure 3 shows the final α-particle kinetic energy E_α, the final fission-fragment energy E_F, and the total energy of the three particles E_T as a function of the initial position X_0 of the α particle along the fission axis. The figure shows the α-particle energy E_α to be strongly dependent on its position, i.e., its initial potential energy, while the dependence of E_F on X_0 is much weaker. The "amplification effect" which causes the final α-particle energy to depend very strongly on its initial kinetic energy as seen in Fig. 2 is not apparent for the variation of the final α-particle energy as a function of its initial potential energy. Yet it may be seen that when the α-particle initial position is near the heavy fragment ($X_0=6\times10^{-13}$ cm, high potential energy), it receives a larger share of the total energy E_T available than when it is near the light fragment ($X_0=20\times10^{-13}$ cm, lower potential energy). As a result E_F is lower for $X_0=6$ than for 20×10^{-13} cm despite the fact that the total energy E_T is higher for the former position. This also explains the fact that the minimum of E_α and E_F occur at different X_0.

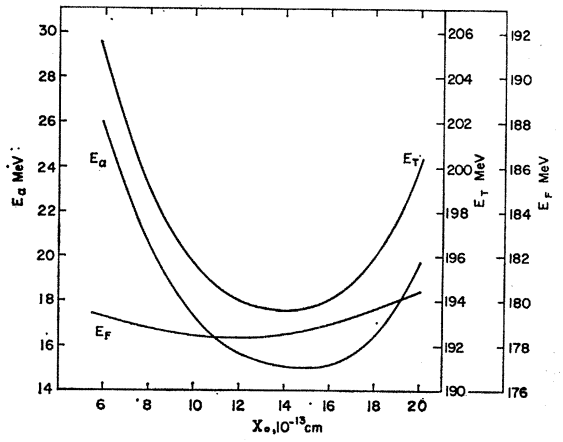

FIG. 3. The final α-particle energy E_α, the final fission fragment energy E_F, and the total energy of the three fragments E_T as a function of the initial distance X_0 of the α particle from the heavy fragment. The values of the initial parameters (except for X_0) are those of Table I.

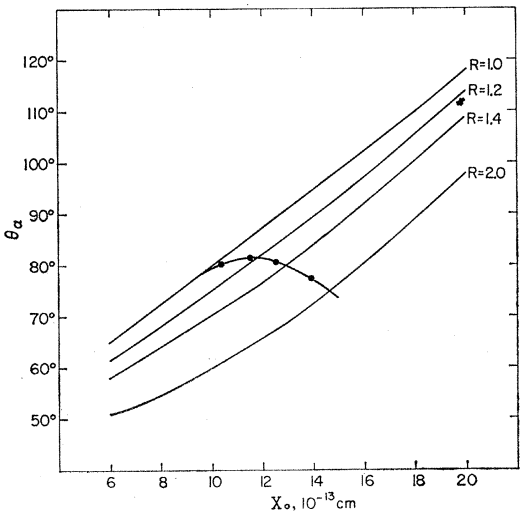

FIG. 4. The final angle θ_α of the α particle with respect to the light fragment as a function of the initial position X_0. The values of the initial parameters (except for X_0) are those of Table I. Also shown are the loci of the most probable values of X_0 as functions of R.

We show in Fig. 4 the final α-particle angle θ_α with respect to the light fragment as a function of the initial position X_0 for four values of the mass ratio R. It is seen that the final angle θ_α is almost linearly dependent on the initial distance X_0 from the heavy fragment. As expected, the angle with respect to the light fragment decreases as the mass ratio increases. (It is seen that the curve $R=1$ has a value $\theta_\alpha>90°$ for the symmetry point $X_0=13\times10^{-13}$ cm and it is not skew-symmetric with respect to the lines $X_0=13\times10^{-13}$ cm and $\theta_\alpha=90°$. This is due to the fact that θ_α is defined as the final angle between the α particle and the light fragment as it is measured experimentally, and hence it includes the recoil angle of the light fragment.)

Based on Figs. 3 and 4, we obtain the final α-particle energy E_α as a function of the final angle θ_α assuming that the variation of both E_α and θ_α is due to the variation of X_0 alone. This graph is shown in Fig. 5 together with the experimental variation E_α (θ_α) as obtained in the preceding paper.[1] It is seen that while qualitatively both curves have the same shape, the angle dependence of the calculated curve is much stronger than that of the experimental one. This discrepancy is in part the result of the assumption that all initial parameters have a single value, whereas, in fact E_α (θ_α) should be calculated for distributions of initial values. Some of these distributions such as $N(R)$ have been measured experimentally, and others must be obtained from calculations such as the present one. However, it seems that even with the true initial conditions there will still remain a discrepancy between the calculated and experimental angle dependence of E_α. This residual discrepancy may

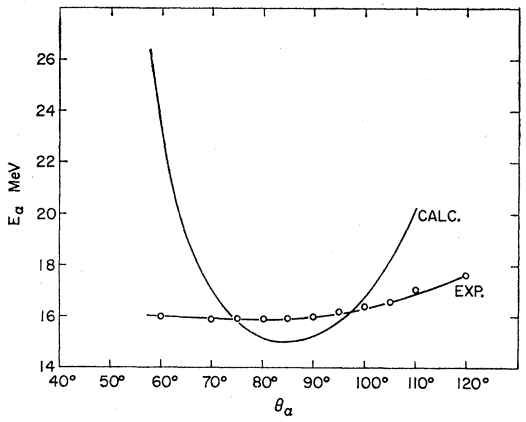

FIG. 5. The calculated α-particle energy E_α as a function of the final angle θ_α, as obtained from Figs. 3 and 4. Also shown is the experimental curve (see Fig. 4 of Ref. 1).

be the result of the three-point-charge approximation of this calculation. A more realistic assumption for the shape of the scissioning nucleus and the resulting fragments may remove it. A quite different way of removing the discrepancy is to assume that the average initial velocity of the α particles which are emitted near the fragments is lower than that of the α particles emitted in the center of the neck. This assumption will be made below.

C. Dependence on the Initial α-Particle Angle θ_0

Figure 6 shows the final α-particle energy E_α as a function of the initial angle θ_0. Angles below $\theta_0=30°$ and above $\theta_0=150°$ are of little practical interest for two reasons: (a) α particles emitted at a small angle with respect to one of the fragments have a large probability of being captured by that fragment. (b) Because of the sin θ dependence of the solid angle, the number of α particles emitted at these angles is quite

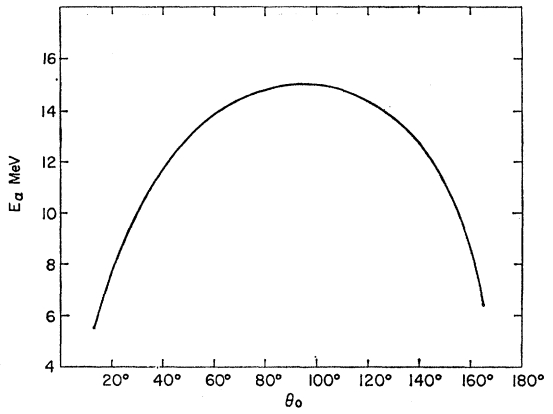

FIG. 6. The final α-particle energy E_α as a function of the initial angle θ_0. The values of the initial parameters (except for θ_0) are those shown in Table I.

small even if isotropic emission is assumed. The small α-particle energy E_α associated with these angles is the result of the reflection which these α particles do suffer. Because of the time dependence of the potential-energy surface which was mentioned above, the almost total reflection of these particles results in low final energies E_α. It is seen from Fig. 6 that in the region of greatest interest, $60°\leq\theta_0\leq120°$, the final energy changes by 1 MeV only. One may, therefore, in general neglect the effect of the initial angle on the final energy E_α.

Figure 7 shows the final angle θ_α as a function of the initial angle θ_0 for three values of the initial energy $E_{\alpha0}$. It is seen that for the initial angles of practical interest, i.e., $30°\leq\theta_0\leq150°$ the final angle θ_α is almost independent of the initial angle θ_0 and of the initial energy $E_{\alpha0}$. Because of the mass ratio of $R=1.4$ assumed for Fig. 7 both $\theta_0=0°$ and $\theta_0=180°$ result in $\theta_\alpha=0°$. For $R=1$, we naturally obtain $\theta_\alpha=180°$ for an initial angle $\theta_0=180°$. However only for values of θ_0 very close to 180° does θ_α show a marked dependence on R.

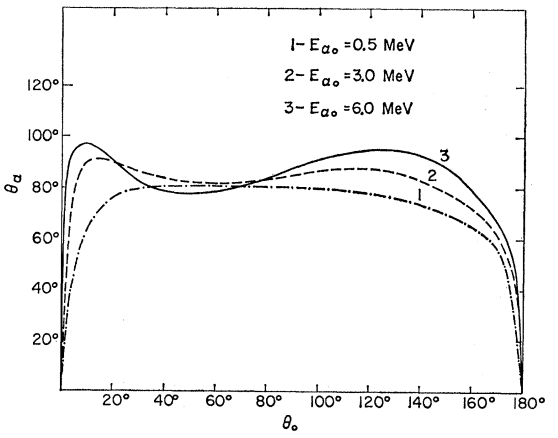

FIG. 7. The final angle θ_α as a function of the initial angle θ_0 for three values of the initial energy $E_{\alpha0}$. All other initial values are those of Table I.

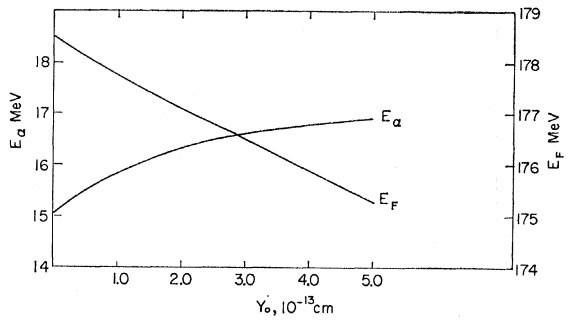

FIG. 8. The final α-particle energy E_α and the final fragment energy E_F as a function of the initial distance Y_0 of the α particle perpendicular to the fission axis. All other initial values are those of Table I.

The calculations shown in Figs. 1–6 were also calculated for $Y_0=5\times10^{-13}$ cm (all other initial parameters as above). The results do not differ markedly from those calculated with $Y_0=0$. The variation of E_α and E_F as a function of Y_0 is seen in Fig. 8 for the initial conditions of Table I except for Y_0. We note that $E_\alpha(Y_0)$ reaches a maximum and then decreases towards the limit $E_\alpha=E_{\alpha0}$ as Y_0 approaches infinity.

We may summarize our analysis of the initial parameters $E_{\alpha0}$, X_0, and θ_0 by concluding that as a first approximation we may *assume θ_α to be independent of $E_{\alpha0}$ and θ_0 and to be a linear function of X_0*. We may further conclude that an initial distribution of $E_{\alpha0}$ and θ_0 alone cannot result in the relatively wide experimentally observed angular distribution $N(\theta_\alpha)$ such as seen in Fig. 2 of the preceding paper. This distribution is predominantly the result of distribution in the initial position X_0 of the α particle.

D. Dependence on the Initial Fragment Velocity V_H and the Initial Fragment Separation D

Figure 9 shows the final α-particle energy E_α as a function of the initial velocity V_H and initial separation D of the fission fragments. It is seen that E_α is an almost linearly decreasing function of both variables.

The question now arises whether a realistic initial distribution of V_H or D (or both) can result in a distribution of the α-particle final energy which is in agreement with the experimental result or whether in addition a distribution of $E_{\alpha0}$, the initial kinetic energy of the α particle, must be assumed. To answer this question, the distribution $N(E_\alpha)$ was calculated assuming all initial parameters to correspond to the values of Table I, except for V_H, which was assumed to vary so as to yield for the total initial kinetic energy of the two fragments E_{F0} a Gaussian distribution:

$$N(E_{F0})_R=C\exp\left[-\frac{1}{2}\frac{(E_{F0}-\bar{E}_{F0})^2}{\sigma^2}\right], \qquad (9)$$

where $\bar{E}_{F0}=39.1$ MeV for $R=1.4$. This value of $\bar{E}_{F0}$ was chosen so as to yield 187 MeV for the total energy of the three-particle system, and the standard deviation was assumed to be $\sigma=12$ MeV. Both values correspond roughly to the experimental values for the total kinetic energy and standard deviation of the three-particle system. The resultant distribution $N(E_\alpha)$ of the α-particle kinetic energy is shown in Fig. 10 together with the experimental curve for this energy range. It is seen that the calculated distribution is much narrower than the experimental one.

A similar calculation was made assuming V_H to be fixed ($V_H=0.5\times10^9$ cm/sec), whereas a Gaussian distribution was assumed for the initial fragment separation D. Again, the mean value and standard deviation were chosen so as to correspond to the experimental values for the total kinetic energy distribution. A curve similar to Fig. 10 was obtained for $N(E_\alpha)$.

The calculations were repeated for $E_{\alpha0}=1.0$ MeV

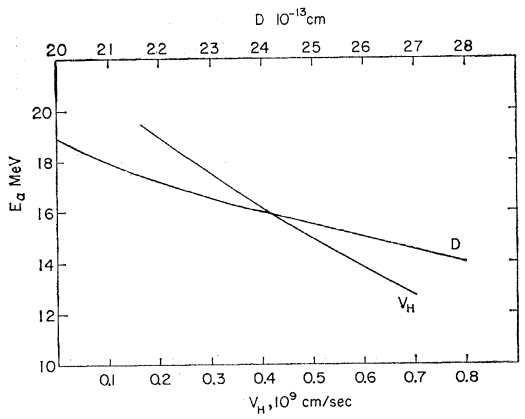

FIG. 9. The final α-particle energy E_α as a function of the initial fragment velocity V_H and the initial fragment separation D. All other initial values are those of Table I.

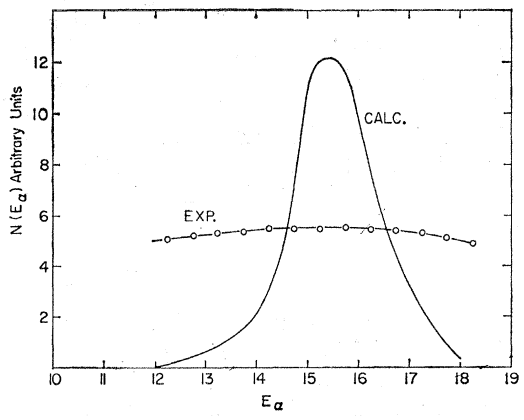

FIG. 10. The calculated distribution $N(E_\alpha)$ assuming the initial fragment kinetic-energy distribution to be given by Eq. (9) and all other initial values to be those of Table I. Also shown is the experimental distribution $N(E_\alpha)$ for the energy range in question (see Fig. 3 of Ref. 1).

with all other input parameters unchanged. Again curves similar to Fig. 10 were obtained.

We may thus conclude that in order to obtain the experimental distributions for the final α-particle energy E_α and the final fragment energy E_F, distributions of substantial width must be assumed for both $E_{\alpha 0}$, the initial α-particle kinetic energy, and V_H or D, or both of the latter variables.

IV. THE KINETIC ENERGIES OF THE α-PARTICLE AND FISSION FRAGMENTS AT THE MOMENT OF SCISSION

In the preceding section we discussed the dependence of the final α-particle kinetic energy and angle on the initial values for the kinematical variables of the system. The set of initial values refers to a time $t=0$ which may be chosen to coincide with any moment in the LRA-fission process equal to or later than the moment of scission. Conversely, if a set of initial values (such as the "standard" set of Table I) gives good agreement with experimental results, this only proves that at a given moment the kinematical variables of the system coincide with these initial conditions. However, it does not give us in general any information about the values of the kinematical variables at the moment of scission. In order to obtain information on the moment of scission, we must find the "earliest" set of initial values which gives agreement with the experimental results for $t=\infty$. It is *a priori* not obvious that an "earliest" set of initial values can be found (except for the trivial one corresponding to zero kinetic energy of the three particles) from the examination of the experimental distributions. Thus clearly no such set can be found for binary fission. However, for LRA fission, information on the moment of scission can be obtained from the correlation between the α-particle energy and the fission fragment kinetic energy and also from the angular distribution of the α particles. This fact makes the investigation of LRA fission of general interest for the physics of fission.

The particular interest in the kinetic energies of the two fragments at the moment of scission is partly due to the fact that the statistical theory of fission[4] assumes this energy to be very small (less than 0.5 MeV), and this theory is not valid if the kinetic energy of the fragments at scission is considerably larger than 1 MeV. Because of the condition that any set of initial values for the kinematical variables should result in final kinetic energies of the fission fragments and the α particle which correspond to the mean experimental values, it suffices to determine the size of one of the variables $E_{\alpha 0}$, V_H, or D at the moment of scission in order to determine the size of the other variables. This is seen in Table II, where we show several sets of initial values which satisfy the above conditions at $t=\infty$, namely $\bar{E}_\alpha=15.9$ MeV and $\bar{E}_F=166.8$ MeV. It is seen that the "standard values" of Table I do roughly correspond to the row of $E_{\alpha 0}=3$ MeV.

TABLE II. Six sets of starting conditions for $E_{\alpha 0}=0.2-5.0$ MeV. The values of the other initial parameters are $R=1.4$, $Y_0=0$, $\theta_0=90°$. All sets satisfy the conditions $E_F\simeq 166.8$ MeV and $E_\alpha\simeq 15.9$ MeV at $\theta_\alpha\simeq 85°$.

$E_{\alpha 0}$ (MeV)	D (10^{-13} cm)	V_H (cm/nsec)	E_{F0} (MeV)	X_0	E_α (MeV)	θ_α (deg)	E_F (MeV)
0.2	20.7	0	0	L	19.5	85	166.7
				M	15.2	85	167.3
				H	24.7	82	166.0
0.5	21.0	0.10	1.8	L	19.7	96	166.2
				M	15.9	85	166.2
				H	25.7	69	164.8
1.0	21.7	0.20	7.3	L	20.0	102	166.4
				M	16.1	85	166.1
				H	26.1	62	165.1
2.0	23.5	0.33	19.8	L	20.3	108	167.2
				M	16.0	85	166.5
				H	26.3	57	166.3
3.0	26.0	0.44	34.4	L	20.3	110	168.5
				M	15.5	86	167.1
				H	26.5	56	167.6
5.0	30.0	0.54	52.3	L	21.7	112	169.0
				M	16.2	87	168.9
				H	28.0	57	168.5

We shall try to establish the size of the three kinematical variables $E_{\alpha 0}$, V_H, and D at the moment of scission from three independent arguments. One argument was first stated by Halpern,[3,5] and we shall discuss it here only briefly: If we assume the α particle to exist as a physical entity in the neck of the fissioning nucleus before scission occurs, it must have a minimum kinetic energy due to the uncertainty principle. If one further assumes the neck to consist of approximately 20 nucleons, one arrives at a value of approximately 4 MeV for the minimum kinetic energy. Finally, if we assume that scission process is so fast that the removal of the nuclear potential does not change the momentum of the α particle (the sudden approximation), we arrive at 4 MeV as the initial kinetic energy of the α particle at the moment of scission. Of the above assumptions the sudden approximation is probably the one which is most open to doubt.

The other two arguments regarding the initial α-particle energy are not based on any assumptions about the dynamics of the LRA-fission process, but try to determine $E_{\alpha 0}$ from the analysis of the experimental results. We show in Table II the final α-particle angle θ_α as a function of the initial α-particle energy $E_{\alpha 0}$ for positions L, M, and H. We see that for values of $E_{\alpha 0}\lesssim 1$ MeV the spread in angle between positions L and H is 40° or less, whereas the experimentally observed angular distribution extends from less than 60° to approximately 110° (see Fig. 2 of the preceding paper). The points L and H, whose distance to the center of the near fragment is only 6×10^{-13} cm, may well be considered extremal points with respect to the emission of α particles, since the "neck" of the scissioning nucleus

[4] P. Fong, Phys. Rev. **102**, 434 (1956).

[5] I. Halpern, in *Symposium on Physics and Chemistry of Fission* (International Atomic Energy Agency, Vienna, 1965), Vol. II, p. 369.

can hardly extend nearer to the fragments. It follows that in order to obtain the experimental angular distribution, the initial energy $E_{\alpha 0}$ of the α particles must be larger than 1 MeV. Since θ_α does not change rapidly above $E_{\alpha 0}=1$ MeV, we are unable to give an upper limit for $E_{\alpha 0}$ from these considerations. The validity of this argument is rather strongly dependent on the extent to which our three-point-charge model can explain the experimentally observed angular and energy distributions.

Our third argument is based on the correlation between E_α and E_F. This subject is discussed in the previous paper and we shall only summarize it briefly: If the initial energies of the three fragments are very small at the moment of scission, the final energies $\bar{E}_F$ and E_α must be highly (negatively) correlated. The larger the initial energies, the smaller the amount of correlation between E_α and $\bar{E}_F$. We define $\bar{E}_F$ as the average kinetic energy of the fragments for a given value of E_α. In Fig. 11 we show two calculated correlation curves between E_α and E_F. Curve A was calculated assuming $D=21\times10^{-13}$ cm, $E_{F0}=1.9$ MeV. Curve B shows this correlation for the initial conditions $D=26\times10^{-13}$ cm, $E_{F0}=35.0$ MeV. The curves were obtained by keeping all initial variables except $E_{\alpha 0}$ fixed and varying $E_{\alpha 0}$ between 0.1 and 0.8 MeV for curve A and between 1.0 and 5.0 MeV for curve B. All initial variables except $E_{\alpha 0}$, D_0, and V_H were those of Table I. For curve A, the value of $E_{\alpha 0}$ corresponding to the average experimental value of $\bar{E}_\alpha=15$ MeV is $\bar{E}_{\alpha 0}=0.3$ MeV, whereas this value is $\bar{E}_{\alpha 0}=3.0$ MeV for curve B. We also show in Fig. 11 the experimentally measured correlation (see Fig. 15 of the preceding paper). It is seen that curve A has the wrong slope, whereas the agreement between curve B and the experimental curve is very good. It may thus be concluded, on the basis of Fig. 11, that the average initial energies of the α particle and fission fragments at the moment of scission are approximately 3 and 40 MeV, respectively. It should, however, be remembered that we assumed fixed values for all initial variables except $E_{\alpha 0}$. Actually, all the initial variables have a finite distribution, and if these initial distributions cause an appreciable correlation between E_α and E_F, our conclusions would be affected. In particular, a strong positive correlation between E_α and E_F could result in the experimental curve, even if $E_{\alpha 0}$ is of the order of 0.1 MeV rather than 1 MeV. Such a positive correlation could be caused by the distributions of the parameters X_0 and D (see Figs. 3 and 9, respectively). However, since the experimental curve was measured at a fixed angle ($\theta_\alpha=90°$), the distribution of X_0 associated with it is presumably very narrow. The positive correlation between E_α and E_F due to the initial distribution in D will be at least partially compensated by the negative correlation due to the initial distribution in V_H.

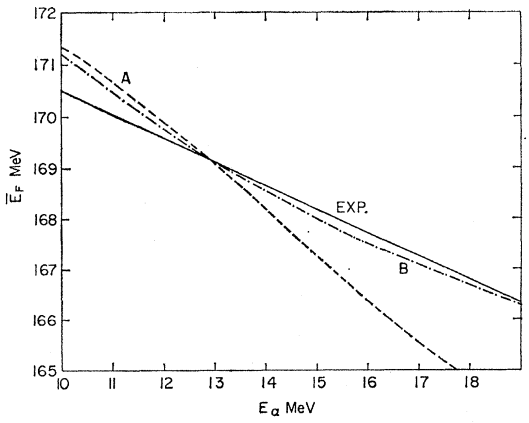

FIG. 11. The calculated correlation between the final α-particle energy $\bar{E}_\alpha$ and the final fragment energy E_F. Curve A corresponds to $D\simeq21\times10^{-13}$ cm, $E_{F0}=1.9$ MeV. Curve B corresponds to $D\simeq26\times10^{-13}$ cm, $E_{F0}=35$ MeV. Curve A is obtained by varying $E_{\alpha 0}$ between 0.1 and 0.8 MeV. Curve B is obtained by varying $E_{\alpha 0}$ between 1.0 and 5.0 MeV. All other initial variables are those of Table I.

In summary, we may say that by three independent methods, we arrive at the conclusion that when scission occurs, the two fragments are already in motion and already have approximately one-half their final velocity ($\frac{1}{4}$ of their final kinetic energy), and the nucleus is highly elongated ($D\simeq26\times10^{-13}$ cm). The initial values of Table I are based on this conclusion. Yet the validity of each of the three arguments is open to some doubt.

V. COMPARISON WITH EXPERIMENTAL DISTRIBUTIONS

In this section we shall try to obtain the distributions of the initial parameters (e.g., $N(E_{\alpha 0})$] which result in final parameter distributions [e.g., $N(E_\alpha)$] in good agreement with the experimental results shown in the preceding paper.[1] However, with a three-point-charge model, we cannot hope to reproduce those variations in the final parameters which are the result of changes in the deformation of the fragments. Experimental evidence for such changes in the deformation as a function of the excitation energy E^* is seen in Figs. 12–14 of the preceding paper. Hence we shall not try to reproduce these results. We shall be mainly interested in reproducing the variation of the average α-particle energy with angle $\bar{E}_\alpha$ (θ_α), the energy spectrum of the α-particles $N(E_\alpha)$, and the dependence of the angular distribution on the α-particle energy $N(\theta_\alpha,E_\alpha)$.

We have seen in Fig. 5 that the calculated value of E_α is a much steeper function of the angle θ_α than the experimental average energy is. In order to obtain agreement between the experimental and calculated curves, we assume that the *initial kinetic energy $E_{\alpha 0}$ is a function of the initial distance X_0*. We assume the initial kinetic-energy distribution at a given point X_0 and a given mass ratio R to be Maxwellian:

$$N(E_{\alpha 0})_{X_0,R}=(\text{const})E_{\alpha 0}\exp[-E_{\alpha 0}/T(X_0)], \quad (10)$$

with

$$T(X_0)=T(M)\left[\frac{U_0(M)}{U_0(X_0)}\right]^2, \tag{11}$$

where $T(M)=\frac{1}{2}\bar{E}_{\alpha 0}(M)=1.5$ MeV.

$U_0(X_0)$ is the potential energy of the α particle at the position X_0 ($Y_0=0$), and $E_{\alpha 0}(M)$ and $U_0(M)$ are the initial kinetic and potential energies of the α particle at position M. No great significance should be attached to the particular X_0 dependence of Eq. (11), and any similar function may give equally good or better agreement with the experimental results. Moreover, even if a unique X_0 dependence could be found for our model, its interpretation in terms of the true dependence of the initial kinetic energy of the α particle on its point of emission in the scissioning nucleus is not obvious. Yet we may conclude from our results that the average initial kinetic energy of the α particle decreases with the increasing initial potential energy, but that the decrease in $E_{\alpha 0}$ does not fully compensate the increase in U_0 as the emission point gets closer to one of the fragments. [Because of the steepness of the function $U_0(X_0)$, the assumption

$$E_{\text{tot}}=U_0(X_0,Y_0)+E_{\alpha 0}(X_0,Y_0)=\text{const}$$

would correspond to a very narrow distribution $N(X_0)$ which cannot reproduce the experimental angular distribution $N(\theta_\alpha)$.]

To a first approximation, the final angle θ_α is only dependent on the initial distance X_0 and the mass ratio R. We can therefore obtain the initial two-dimensional distribution $N(X_0,R)$ from the experimentally observed, angular distribution $N(\theta_\alpha,R)$ as given by Fig. 10 of the preceding paper.[1]

$$N(X_0,R)=N(\theta_\alpha,R)\frac{\partial\theta_\alpha}{\partial X_0}(R), \tag{12}$$

where $(\partial\theta_\alpha/\partial X_0)$ (R) is obtained from Fig. 4. Since the effect of the variation of E_{F0} and D on the final distributions is similar (see Fig. 9), we arbitrarily assume D to be fixed ($D=26\times10^{-13}$ cm) and E_{F0} to have a finite initial distribution in the form of Eq. (9). In that equation σ is assumed to be 12.0 MeV, whereas E_{F0} is chosen to be a linear function of R.

$$\bar{E}_{F0}(R)=28.0+8.0R \text{ MeV}. \tag{13}$$

This function yields good agreement between the calculated and experimental values of $\bar{E}_F(R)$, the average final kinetic energy of the fission fragments (see Fig. 7 of the preceding paper). The initial parameters Y_0 and θ_0 were assumed to be fixed ($Y_0=0$ and $\theta_0=90°$) since their variation has little effect on the final distribution. Combining Eqs. (9), (10), (12), and (13), we thus obtain a four-dimensional initial distribution $N(X_0,R,E_{\alpha 0},E_{F0})$. From this distribution we obtain the final ("experimental") distribution $N(\theta_\alpha,E_\alpha,R)$,

$$N(\theta_\alpha,E_\alpha,R)=\int N(X_0,R,E_{\alpha 0},E_{F0})\frac{\partial(X_0,E_{F0})}{\partial(\theta_\alpha,E_\alpha)}dE_{\alpha 0}. \tag{14}$$

The Jacobian may be approximated by

$$\frac{\partial(X_0,E_{F0})}{\partial(\theta_\alpha,E_\alpha)}\simeq\frac{\partial X_0}{\partial\theta_\alpha}\frac{\partial E_{F0}}{\partial E_\alpha}, \tag{15}$$

since θ_α is essentially independent of E_{F0}. For a fixed mass ratio R, the initial distribution is the product of two independent parts

$$N(X_0,E_{\alpha 0},E_{F0})_R=N(X_0,E_{\alpha 0})_R N(E_{F0})_R, \tag{16}$$

where the two distributions on the right side of Eq. (16) are given by Eqs. (9), (10), (12), and (13). The final distribution $N(\theta_\alpha,E_\alpha)_R$ is given by

$$N(\theta_\alpha,E_\alpha)_R=\int N(X_0,E_{\alpha 0})_R N(E_{F0})_R \times\left(\frac{\partial X_0}{\partial\theta_\alpha}\frac{\partial E_{F0}}{\partial E_\alpha}\right)_R dE_{\alpha 0}. \tag{17}$$

In Figs. 12–14, we show this function for the values $R=1.0$, $R=1.4$, and $R=1.6$. In each figure the calculated angular distribution $N(\theta_\alpha)$ is plotted for three intervals of the kinetic energy E_α. The qualitative agreement with the experimental curves (Fig. 11 of the preceding paper) is very good.[6] The α-particle energy spectrum at a given angle (and given R) is also

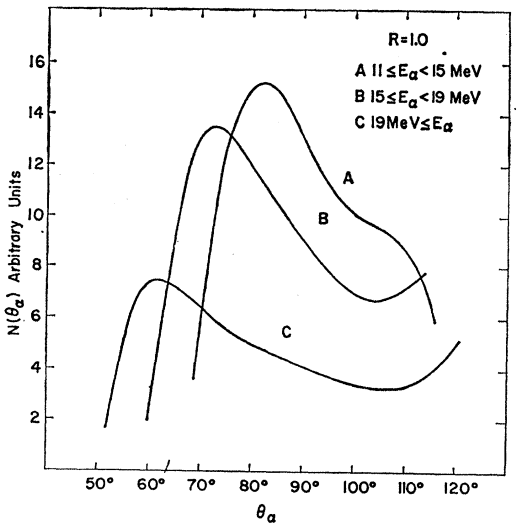

FIG. 12. The calculated angular distribution of the α particle for three intervals of the α-particle kinetic energy. $R=1.0$.

[6] The renewed rise of curve C in Fig. 14 near $\theta_\alpha=60°$ is believed to be the result of an overestimate of the α-particle recoil effect in Fig. 10 of the preceding paper. See also Appendix II of that paper. The same explanation also holds for the bumps in curve B of Fig. 14 near 60° and in Fig. 12 near 120°.

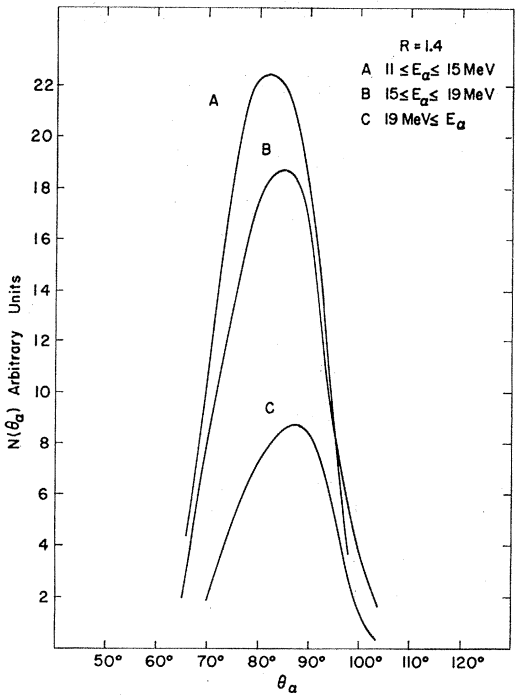

FIG. 13. The calculated angular distribution of the α particles for three intervals of the α-particle kinetic energy. $R=1.4$.

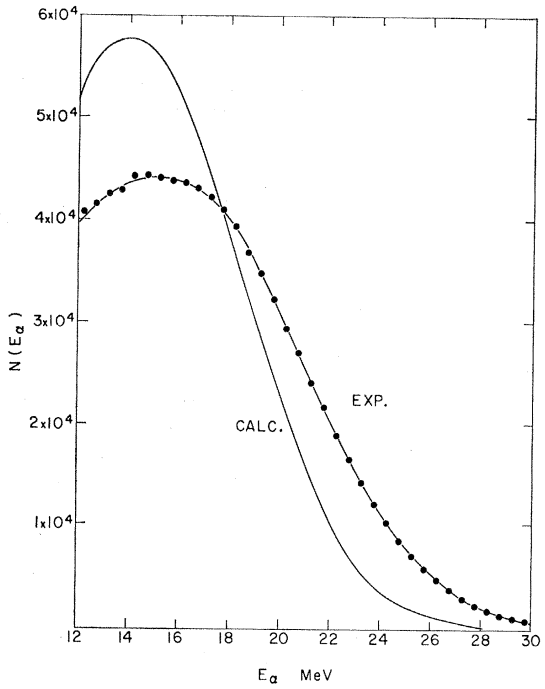

FIG. 15. The uncorrelated α-particle energy spectrum for $R=1.4$. Also shown is the experimental result (see Fig. 3 of Ref. 1). The curves are normalized to the same area.

expressed by Eq. (17), and the uncorrelated ("isotropic") spectrum is obtained by integrating over $\cos\theta_\alpha$:

$$N(E_\alpha)_R=\frac{1}{2}\int_{-1}^{+1} N(\theta_\alpha,E_\alpha)_R d(\cos\theta_\alpha). \qquad (18)$$

Figure 15 shows this spectrum for $R=1.4$ together with the experimental curve for all R (see also Fig. 3 of the preceding paper). The calculated curve has been normalized to the same area as that of the experimental curve. The agreement is again quite good, although the calculated curve seems to be somewhat narrower and shifted by approximately 1 MeV towards lower energies. (The α-particle energy spectrum is not very R-dependent and similar agreement would have been obtained for the calculated curve integrated over all R). The average α-particle energy as a function of θ_α is given by

$$\bar{E}_\alpha(\theta_\alpha)_R=\int E_\alpha N(\theta_\alpha,E_\alpha)_R dE_\alpha. \qquad (19)$$

This function is shown in Fig. 16 for $R=1.0$, $R=1.4$,

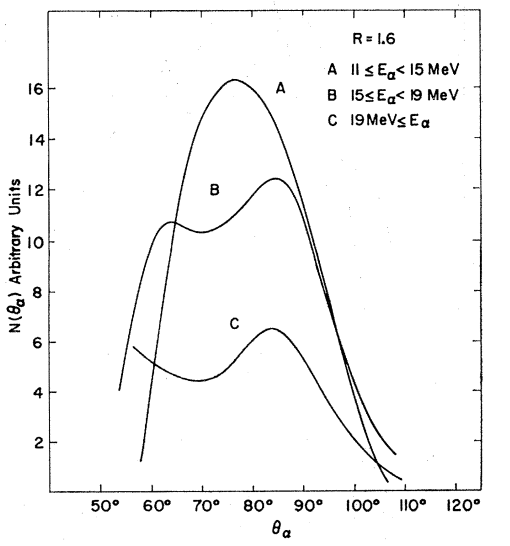

FIG. 14. The calculated angular distribution of the α particles for three intervals of the α-particle kinetic energy. $R=1.6$.

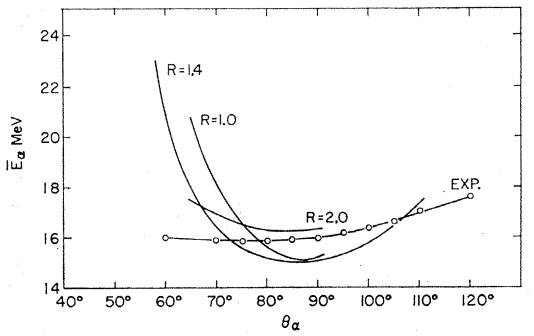

FIG. 16. The calculated average α-particle energy as a function of the α-particle angle for $R=1.0$, $R=1.4$, and $R=2.0$. Also shown is the experimental curve which is integrated over all values of R (see Fig. 4 of Ref. 1).

and $R=2.0$ together with the experimental curve for all R. It is seen that although the agreement with the experimental curve is improved as compared to Fig. 5, the calculated curves are still a steeper function of the angle θ_α than the experimental curve. A stronger X_0 dependence of $\bar{E}_{\alpha 0}$ than that given by Eq. (11) would further improve the agreement.

If we wish to integrate over all R, we must use the four-dimensional distribution $N(X_0,R,E_{\alpha 0},E_{F0})$. This was done in order to obtain the α-particle angular distribution as a function of E_α:

$$N(\theta_\alpha,E_\alpha)=\int N(X_0,R,E_{\alpha 0},E_{F0})\frac{\partial X_0}{\partial \theta_\alpha}\frac{\partial E_{F0}}{\partial E_\alpha}dE_{\alpha 0}dR. \quad (20)$$

The angular distribution integrated over all R is shown in Fig. 17 for four intervals of the kinetic energy E_α. The calculated curves reproduce the main feature of the experimental results (Fig. 9 of the preceding paper), namely, the flattening of the angular distribution as E_α increases until the curve changes from convex to concave at $E_\alpha>23$ MeV.

The distribution $N(X_0)$ may be obtained by integrating Eq. (12) over all values of R. The result is shown in Fig. 18. The distribution is roughly symmetrical with respect to the center of the scission axis ($X_0=13\times10^{-13}$ cm) and falls off to zero close to points H and L ($X_0=6\times10^{-13}$ cm and 20×10^{-13} cm, respectively).

With the aid of Eq. (12) and the experimental distribution $N(\theta_\alpha,R)$ (Fig. 10 of the preceding paper), we can also obtain the most probable initial distance X_0 of the α particle (or, equivalently, the scission point) from the heavy fragment as a function of R, assuming the "standard" initial values (Table I) for D, V_H, Y_0, $E_{\alpha 0}$, and θ_0. The loci of the most probable values of X_0 as a function of R are shown in Fig. 4. It is seen that the most probable initial distance moves from

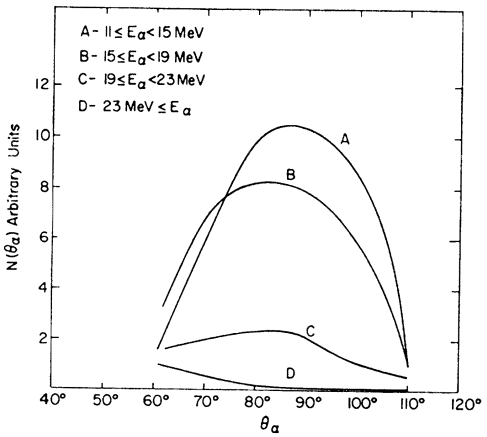

FIG. 17. The calculated angular distribution of the α particles for four intervals of the α-particle kinetic energy.

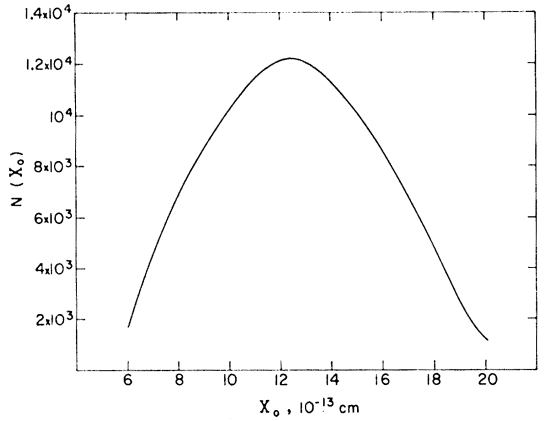

FIG. 18. The calculated distribution $N(X_0)$ based on the experimental results of Ref. 1.

$X_0\simeq10\times10^{-13}$ cm for $R=1$ to $X_0\simeq15\times10^{-13}$ cm for $R=2$.

We conclude that using the above assumptions [Eqs. (9)–(13)], with regard to the initial distribution $N(X_0,R,E_{\alpha 0},E_{F0})$, our model reproduces the main features of those experimental distributions which are not the results of changes in the deformation of the fragments. However, this should not be taken as proof that our initial distribution is indeed an accurate description of the true initial distribution. In particular, the distribution $N(X_0)$ was obtained from the experimental distributions $N(\theta_\alpha,R)$ by a simple transformation which is only correct for our three-charge-point model. The true distribution $N(X_0)$ quite probably differs substantially from the one shown here.

VI. CONCLUSIONS

We have shown that with the initial distribution $N(X_0,R,E_{\alpha 0},E_{F0})$ of Sec. V, the three-point-charge model can reproduce reasonably well the experimental angular and energy distributions of the α particles in LRA fission. We are unable to reproduce the experimental variation of the α-particle distribution as a function of the kinetic energy of the fission fragments (or, equivalently, their excitation energy). As discussed in the preceding paper, the latter variations are probably due to the change in the fragment distortion as a function of their excitation energy, and hence cannot be expected to be reproduced by a three-point-charge model. A more sophisticated model for the fissioning nucleus may not only be able to reproduce these variations, but presumably also improve the agreement between those calculated and experimental results which are not related to changes in the excitation energy.

It was shown that for the three-point-charge model, the final angle θ_α of the α particle depends, to a first approximation, only on its point of emission, and hence by a simple transformation of variables, one obtains

the initial position (i.e., scission point) distribution from the experimental angular distribution. This fact was used in the determination of the initial distribution in Sec. V. In the same fashion, we obtained the average emission point $\bar{X}_0$ as a function of R from the experimental angular distributions for various values of R which were shown in Fig. 10 of the preceding paper. For the three-point-charge model $\bar{X}_0$ varies from 10×10^{-13} cm from the center of the heavy fragment (for $R=1$) to 11×10^{-13} cm from the center of the light fragment (for $R=2$). While these values of $\bar{X}_0$ may be substantially different for the physical scissioning nucleus, our calculation nevertheless supports the view expressed in the above-mentioned paper that the scission point moves closer *to the light fragment as R increases*, and that the variation in $\bar{X}_0$ as a function of R amounts to a substantial part of the distance between the centers of the fragment at the moment of scission.

We have presented additional support for the argument first given by Halpern[3,5] that, at the moment of scission, the fragments have already acquired a substantial part of their kinetic energy. Our calculation shows that good agreement with the experimental results is obtained if we assume that the average energy of the α particle at the moment of scission is $\bar{E}_{\alpha 0}\simeq3$ MeV, the average total kinetic energy of the two fragments is $\bar{E}_{F0}\simeq40$ MeV, and the average distance between the centers of the two fragments is $\bar{D}\simeq26\times10^{-13}$ cm. These conclusions contradict the assumption of the statistical theory of fission[4] that at the moment of scission the kinetic energy of the two fragments is negligible (less than 1.0 MeV). It may of course be argued that our conclusions pertain only to LRA fission and that in binary fission the scission moment occurs much earlier, when the kinetic energy of the fission fragments is indeed still negligible. Such a situation is unlikely in view of the great similarity of the two processes, as seen in the preceding paper. It would leave unexplained the fact that LRA fission is also asymmetric.

ACKNOWLEDGMENTS

The authors would like to thank L. Meilen and M. Weinstein for their help in the computations. They would also like to thank Dr. J. R. Nix for many valuable comments.

PHYSICAL REVIEW VOLUME 156, NUMBER 4 20 APRIL 1967

(d,p) and (d,t) Reactions on the Isotopes of Tin*

EDWARD J. SCHNEID,† ANAND PRAKASH,‡ AND BERNARD L. COHEN
University of Pittsburgh, Pittsburgh, Pennsylvania

(Received 15 March 1965; revised manuscript received 28 November 1966)

Energy levels up to ~4-MeV excitation energy are studied using the (d,p) and (d,t) reactions. Spectroscopic factors for most of the levels are obtained with the aid of distorted-wave Born-approximation (DWBA) calculations. The $\frac{7}{2}^+$ state is not identified in Sn^{123} and Sn^{125}. Several new $l=2$ states are identified as well as several $l=1$ and $l=3$ states belonging to the 82–126-neutron shell. A renormalization of the DWBA absolute cross sections is performed to eliminate systematic inconsistencies in the sum of $U_j^2+V_j^2$. The factors of renormalization are found to be within the well-known uncertainties of the DWBA calculations. The values of relative single-particle energies $(\epsilon_j-\epsilon_{5/2})$ are calculated both from the occupation numbers (U_j^2 or V_j^2) and from the single-quasiparticle energies (E_j) using pairing theory. The results are in disagreement by as much as 1 MeV or more. From the reactions on the odd isotopes, spin and parity information is obtained for many states in Sn^{114}, Sn^{116}, Sn^{118}, and Sn^{120}.

I. INTRODUCTION

THE (d,p) and (d,t) "stripping" reactions have been found to be very useful for shell-model studies of nuclear structure. The excitation energies and transition strengths of the nuclear levels excited in these reactions yield direct information about the excitation energies and the occupation numbers of the single-particle shell-model states.

The tin isotopes are particularly well suited to provide information about the 50–82-neutron shell. In tin, the protons form a closed shell ($Z=50$), making the neutron spectrum relatively simple. The large number of stable isotopes also provide many targets, so trends can be observed as the neutron shell is filling.

In a previous work,[1] the nuclear structure of the tin isotopes was investigated. The work reported here represents an improvement over that study in that: (1) thinner targets have been obtained[2] which allows a

Work performed at the Sarah Mellon Scaife Radiation Laboratory and supported by the National Science Foundation.

† Present address: Rutgers, The State University, New Brunswick, New Jersey.

‡ Present address: Yale University, New Haven, Connecticut.

[1] B. L. Cohen and R. E. Price, Phys. Rev. **121**, 1441 (1961).

[2] The tin isotopes as self-supporting foils were obtained from the stable Isotopes Division, Oak Ridge National Laboratory, Oak Ridge, Tennessee.